

Magnetic fields in cosmic particle acceleration sources

Andrei M. Bykov · Donald C. Ellison ·
Matthieu Renaud

Received: date / Accepted: date

Abstract We review here some magnetic phenomena in astrophysical particle accelerators associated with collisionless shocks in supernova remnants, radio galaxies and clusters of galaxies. A specific feature is that the accelerated particles can play an important role in magnetic field evolution in the objects. In particular, we discuss a number of cosmic-ray (CR) driven, magnetic field amplification processes that are likely to operate when diffusive shock acceleration (DSA) becomes efficient and nonlinear. The turbulent magnetic fields produced by these processes determine the maximum energies of accelerated particles and result in specific features in the observed photon radiation of the sources. Equally important, magnetic field amplification by the CR currents and pressure anisotropies may affect the shocked gas temperatures and compression, both in the shock precursor and in the downstream flow, if the shock is an efficient CR accelerator. Strong fluctuations of the magnetic field on scales above the radiation formation length in the shock vicinity result in intermittent structures observable in synchrotron emission images. The finite size twinkling, intermittent structures – dots, clumps, and filaments – are most apparent in the cut-off region of the synchrotron spectrum. Even though these X-ray synchrotron structures result from turbulent magnetic fields, they could still be highly polarized providing an important diagnostic of the spectrum of the turbulence. We discuss

Andrei Bykov
A.F.Ioffe Institute for Physics and Technology, 194021 St. Petersburg, Russia,
also St. Petersburg State Politechnical University E-mail: byk@astro.ioffe.ru

Donald C. Ellison
Physics Department, North Carolina State University, Box 8202, Raleigh, NC
27695, USA E-mail: don_ellison@ncsu.edu

Matthieu Renaud
Laboratoire de Physique Theorique et Astroparticules (LPTA) Universite
Montpellier II, France E-mail: mrenaud@lpta.in2p3.fr

both the thermal and non-thermal observational consequences of magnetic field amplification in supernova remnants and radio-galaxies. Resonant and non-resonant CR streaming instabilities in the shock precursor can generate mesoscale magnetic fields with scale-sizes comparable to supernova remnants and even superbubbles. This opens the possibility that magnetic fields in the earliest galaxies were produced by the first generation Population III supernova remnants and by clustered supernovae in star forming regions.

Keywords radiation mechanisms: non-thermal—X-rays: ISM— (ISM:) supernova remnants—clusters of galaxies—shock waves—magnetic fields

1 Introduction

Particle acceleration takes place in many active astrophysical objects of very different nature and scales. Magnetic fields play the central role in charged particle acceleration either as a intermediary between the plasma flows and energetic particles, as is the case for Fermi acceleration (e.g., in collisionless shocks), or as a source of free energy to be converted into energetic particles (i.e., magnetic field reconnection processes).

The existence of the highly amplified magnetic fields in the range of 0.1-1 mG in the shells of young supernova remnants (SNRs) was established assuming equipartition between relativistic particles and magnetic fields in the synchrotron radio emitting shells (see e.g., Ginzburg and Syrovatskii 1964, and the references therein). The topology of the magnetic field in SNRs inferred from the observations of synchrotron emission differ strongly between young and old SNRs. Radio polarization studies reveal super-adiabatic magnetic field amplification and a net radial orientation of the magnetic fields in young SNRs, while it is often just shocked interstellar field, mainly tangential, in old SNRs (e.g., Milne 1990). Milne has also pointed out that as the resolution increases, the polarization structure becomes more complex.

A pixel-by-pixel map of Faraday rotation has been produced applying rotation measure (RM) synthesis to the data observed with the *Australia Telescope Compact Array*, for the entire supernova remnant G296.5+10.0 by Harvey-Smith et al. (2010). A highly ordered rotation measure structure, with an anti-symmetric rotation measure pattern, was observed. The authors propose that the observed rotation measures are the imprint of an azimuthal magnetic field in the stellar wind of the progenitor star. A swept-up magnetized wind from a red supergiant can produce an azimuthal pattern of the magnetic field at large distances from the star and can naturally produce the observed anti-symmetric RM pattern. Supernova expansion into such a wind could account for the apparent bilateral structure of the SNR's radio and X-ray morphologies. In the case of SN1006, a comparison between observed and synthesized radio maps, making different assumptions about the dependence of electron injection efficiency on the shock obliquity, allowed Petruk et al. (2009) to constrain possible nonthermal electron injection models.

A number of possible amplification mechanisms were considered. Rayleigh-Taylor instabilities in the shell have been considered for many years as a

potential source of the turbulent magnetic fields. The Rayleigh-Taylor instability at the interface of the ejecta and the shocked ambient medium was proposed to explain these observations. Jun and Norman (1996) performed multi-dimensional MHD simulations of the instability in the shell and its effect on the local magnetic field. They found that the evolution of the instability is very sensitive to the deceleration of the ejecta and the evolutionary stage of the remnant. The Rayleigh-Taylor and Kelvin-Helmholtz instabilities amplify ambient magnetic fields in the simulations locally by as much as a factor of 60 around dense fingers due to stretching, winding, and compression. Globally, the amount of magnetic-field amplification was nevertheless low and the magnetic energy density reaches only about 0.3% of the turbulent energy density at the end of simulation. Strong magnetic field lines draped around the fingers produce the radial B-vector polarization. Magnetic Rayleigh-Taylor instabilities in three dimensions were simulated by Stone and Gardiner (2007), with a focus on the nonlinear structure and evolution that results from different initial field configurations. They found that strong magnetic fields do not suppress the instability but reduce mixing between the heavy and light fluids and cause the rate of growth of bubbles and fingers to increase in comparison to hydrodynamics. Schure et al. (2009) suggested that higher compression ratios and additional turbulence due to the dominant presence of CRs can be important in attempts to reproduce the observed magnetic field morphology with the Rayleigh-Taylor instability simulations. Both numerical simulations and laboratory laser experiments are ongoing to study the RayleighTaylor instability problem. The possible effects of magnetic fields on laser experiments of RayleighTaylor instabilities in supernova-like setups was discussed recently by Fryxell et al. (2010). Comparing numerical simulations, as well as experimentally using the Omega Laser at the University of Rochester, the authors discussed a possibility that the morphology of the instability is significantly altered by the generation of very strong magnetic fields during the laser experiments.

On the other hand, Chevalier (1977) shown that radio observations of Tycho's supernova remnant indicated the presence of a collisionless shock wave undergoing turbulent magnetic field amplification by a factor of about 20. He noted that the amplification resembled some phenomena in heliospheric collisionless shocks. In fact, direct support for the self-generation of MHD turbulence has been seen in heliospheric shocks, e.g., Bamert et al. (2004, 2008). In the upstream region of a shock associated with the Bastille Day coronal mass ejection, the excitation of hydromagnetic waves with power spectral density levels well above the levels in the ambient solar wind were observed by Bamert et al. (2004) with the magnetometer on board the *Advanced Composition Explorer*. Achterberg et al. (1994) set upper limits on the scattering mean free paths of radio emitting electrons in front of supernova remnant shock fronts using high-resolution radio observations of four Galactic supernova remnants. They found that, for the sharpest synchrotron radio rims, the mean free path is typically less than one percent of that derived for cosmic rays of similar rigidity in the interstellar medium, implying that enhanced hydromagnetic wave intensity is generated by diffusive shock acceleration.

Recent observations of X-ray synchrotron radiation from several young SNRs revealed thin X-ray filaments in the vicinity of blast waves. This provides indirect, but rather strong evidence for strong super-adiabatic magnetic field amplification (MFA) in the blast wave associated with CR production (see e.g., Vink and Laming 2003, Bamba et al. 2005, 2006, Uchiyama et al. 2007, Patnaude and Fesen 2008, Reynolds 2008, Vink 2008). The synchrotron filamentary structures could be due to a narrow spatial extension of the highest energy electron population in the shock acceleration region limited by rapid synchrotron energy losses. In this case, strong magnetic field amplification in the shock vicinity is required to match the observed thickness of the non-thermal filaments (e.g., Vink and Laming 2003, Bamba et al. 2005), thus supporting the case for highly efficient DSA. An alternative interpretation, that the observed narrow filaments are limited by magnetic field damping and not by the energy losses of the radiating electrons, has also been proposed (see Pohl et al. 2005, Butt et al. 2008, for example). Cassam-Chenaï et al. (2007, 2008) have studied this effect in detail for Tycho's SNR and SN1006.

Diffusive shock acceleration is a very promising mechanism for producing superthermal and relativistic particles in a wide range of astrophysical objects ranging from the Earth bow shock (e.g., Ellison et al. 1990) to shocks in galaxy clusters (Blandford and Eichler 1987, Jones and Ellison 1991, Malkov and Drury 2001, Bykov et al. 2008a). This mechanism is believed to be efficient (e.g., Helder et al. 2009) and capable of producing CRs to energies well above 10^{15} eV in young SNRs (e.g., Ptuskin et al. 2010), and even higher in active radio-galaxies such as Cen A (see, for example, Croston et al. 2009).

Fast and efficient DSA demands that particles are multiply scattered by magnetic fluctuations in the shock vicinity. The amplitude of the required MHD turbulence is substantially higher than the ambient MHD turbulence suggesting that the turbulence is generated by the shock. In order for DSA to accelerate particles to high energies, the energetic particles must be able to interact with magnetic turbulence over a broad wavelength range. The weakly anisotropic distribution of accelerated particles, is believed capable of producing this turbulence in a symbiotic relationship where the magnetic turbulence required to accelerate the CRs is created by the accelerated CRs themselves. In efficient DSA, this wave-particle interaction can be strongly nonlinear where CRs modify the plasma flow and the specific mechanisms of magnetic field amplification.

2 Magnetic field amplification by CR-driven instabilities

The non-equilibrium distributions of accelerated particles in efficient DSA are believed capable of producing magnetic turbulence and magnetic field amplification. For the forward shock in a young, isolated SNR, the accelerated CR pressure can be a sizeable fraction of the shock ram pressure and far exceed the background plasma pressure. The anisotropic distribution of CRs in the shock precursor results in ponderomotive forces on the background plasma that can cause the amplification of magnetic fluctuations in a certain

wavevector range and polarization. We briefly discuss in section 2.1 the kinetic background for the description of this CR anisotropy and then outline a number of instabilities related to the anisotropic CR distributions.

2.1 Anisotropic CR distribution in DSA

First-order Fermi acceleration (also called diffusive shock acceleration) of CRs by non-relativistic magnetized flows, is characterized by a nearly isotropic CR momentum distribution in a broad energy range. Two notable exceptions to this are injected, barely superthermal particles, and the highest energies CRs. The CR distribution is formed by the multiple scattering of charged particles across the shock by magnetic fluctuations over a wide dynamic range. Cosmic-ray particle dynamics in DSA is governed by electro-magnetic fields both regular and stochastic. The distribution function of energetic particles, $f(\mathbf{r}, \mathbf{p}, t) = \langle F(\mathbf{r}, \mathbf{p}, t) \rangle_c$, averaged over electro-magnetic fluctuations with scales below some value l_c , appropriate for a particular problem, satisfies the kinetic equation

$$\frac{\partial f}{\partial t} + \mathbf{v} \cdot \frac{\partial f}{\partial \mathbf{r}} + e\mathbf{E} \cdot \frac{\partial f}{\partial \mathbf{p}} - \frac{ec}{\mathcal{E}} \mathbf{B} \cdot \hat{\mathcal{O}} f = \hat{I}_c [f], \quad (1)$$

where $\hat{\mathcal{O}}$ is the momentum rotation operator, defined by

$$\hat{\mathcal{O}} = \mathbf{p} \times \frac{\partial}{\partial \mathbf{p}}, \quad (2)$$

\mathcal{E} is the particle energy, and $\mathbf{E} = \langle \mathbf{E}_0 \rangle_c$ and $\mathbf{B} = \langle \mathbf{B}_0 \rangle_c$ are the electric and magnetic fields averaged over electro-magnetic fluctuations with scales below l_c . The fluctuating parts of the electromagnetic fields are $\mathbf{b} = \mathbf{B}_0 - \langle \mathbf{B}_0 \rangle_c$ and $\mathbf{e} = \mathbf{E}_0 - \langle \mathbf{E}_0 \rangle_c$. The fields are self-consistent since the sources in Maxwell's equations include the CR currents determined by $F(\mathbf{r}, \mathbf{p}, t)$. We should stress here that it is not trivial to get a closed system of equations for the averaged distribution function $f(\mathbf{r}, \mathbf{p}, t) = \langle F(\mathbf{r}, \mathbf{p}, t) \rangle_c$ since the higher order moments of F may contribute through $\langle \mathbf{b}(\mathbf{r}, t) F(\mathbf{r}, \mathbf{p}, t) \rangle_c$ and $\langle \mathbf{e}(\mathbf{r}, t) F(\mathbf{r}, \mathbf{p}, t) \rangle_c$. In fact, even the existence of a well defined averaging procedure, and the averages themselves, is assumed rather than proved.

The collision operator

$$\hat{I}_c [f] = -Ze \langle \mathbf{e} \cdot \frac{\partial F}{\partial \mathbf{p}} - \frac{c}{\mathcal{E}} \mathbf{b} \cdot \hat{\mathcal{O}} F \rangle_c, \quad (3)$$

is, in general, a nonlinear operator if the effect of energetic particles on the electromagnetic fields is non-negligible.

Different approaches are used to get a closed analytic expression for $\hat{I}_c [f]$ including Fokker-Planck type equations and quasi-linear theory (see e.g., Toptygin 1985, Blandford and Eichler 1987, Berezhinskii et al. 1990, Schlickeiser 2002). The simplest case for the collision operator can be deduced from Eq. (3) for particles scattered by magnetic fluctuations with scales, l_c , smaller

than the particle gyroradius, $r_g = cp/eB$, in the total magnetic field B (random plus coherent). In the high-energy limit, $r_g \gg l_c$, the particle momentum change over the field correlation length l_c is small ($\propto l_c/r_g$) and the scattering rate in Eq. (3) reduces to $v/2\Lambda(p)\hat{\mathcal{O}}^2$ with $\Lambda(p) = gR_{\text{st}}^2(\mathbf{p})/l_c$. Here, $R_{\text{st}}(p)$ is the particle gyroradius in the stochastic magnetic field, and g is a numerical factor depending on the short-scale fluctuation spectral index. The strong momentum dependence, $\Lambda \propto p^2$, makes this scenario unfavorable for confining and accelerating high-energy particles in DSA.

It is important to note that $\hat{\mathcal{O}}^2$ can be reduced to the angular part of the Laplace operator with well-known spherical harmonics as the eigenfunctions. The high-energy asymptotic range is valid even in the case of strong (but quasi-static) magnetic fluctuations of amplitudes larger than the mean magnetic field. However, for particles of intermediate and low energies, with $r_g \lesssim l_c$ and scattered by strong magnetic fluctuations, the collision operator is no longer simple and only some phenomenological scheme like the *relaxation time approximation* can be used. These schemes do not have a microscopic justification.

The momentum distribution of accelerated particles, $f(\mathbf{r}, \mathbf{p}, t)$, of a weakly anisotropic distribution can be presented as

$$f(\mathbf{p}) = \frac{n_{\text{cr}}}{4\pi} N(p) [1 + \delta_{\text{a}}(\mathbf{p})], \quad (4)$$

where n_{cr} is the CR number density, $N(p)$ is the isotropic and $\delta_{\text{a}}(\mathbf{p})$ is the anisotropic part of the distribution function defined to satisfy

$$\int \delta_{\text{a}}(\mathbf{p}) d\Omega_{\mathbf{p}} = 0, \quad \int f(\mathbf{p}) p^2 dp d\Omega_{\mathbf{p}} = n_{\text{cr}}.$$

Due to CR particle scattering by magnetic fluctuations of different scales, the distribution function is nearly isotropic on scales larger than the CR mean free path, $\Lambda(p)$, and, therefore, its anisotropic part is small, i.e., $\delta_{\text{a}}(\mathbf{p}) \ll 1$ on scales $k\Lambda(p) < 1$. The actual angular dependence of $\delta_{\text{a}}(\mathbf{p})$, and the momentum dependence of $\Lambda(p)$, are determined by the exact form of the collision operator, the structure of regular fields, and the boundary conditions. It can be presented in the spherical harmonic expansion

$$\delta_{\text{a}}(\mathbf{p}) = \sum_{l,m} \Delta_{l,m}(p) Y_{l,m}(\vartheta, \varphi), \quad |m| \leq l, \quad (5)$$

where ϑ and φ are the pitch and azimuthal angles of the particle momentum, correspondingly. Since the isotropic part of the distribution function is separated from the anisotropic part in Eq. (4), $\Delta_{0,0} = 0$. The current-type anisotropy that is determined by $\Delta_{1,m} < 1$, is usually considered to be the dominant term. That results in the standard diffusion approximation and the transport equation for the isotropic part $N(\mathbf{r}, p, t)$. In the case of a high-energy particle scattering off of small-scale fluctuations, $r_g \gg l_c$, the spherical functions are the eigenfunctions of the collision operator since $\hat{\mathcal{O}}^2 Y_{l,m} = -l(l+1)Y_{l,m}$. In that case, indeed, $\Delta_{2,m} \sim \Delta_{1,m}^2$. However, the high multipole components of the distribution can be substantial in the case

of anisotropic scattering, or in plasma flows with a complex structure of quasi-regular magnetic fields (e.g., in the presence of regular or stochastic magnetic traps). In the latter case one can expect $\Delta_{2,m} \sim \Delta_{1,m}$ and the transport equation for the isotropic part of the distribution function $N(\mathbf{r}, p, t)$ can differ from the standard advection-diffusion equation that is used in the analytic DSA models.

Standard analytic DSA models use a simplified description of particle diffusion. Generally, the diffusion approximation is made where it is assumed that a small anisotropy of the momentum distribution can be completely described by the CR current and higher moments of the momentum angular distribution can be neglected (see e.g., Blandford and Eichler 1987, Jones and Ellison 1991, Malkov and Drury 2001). Then, further assuming that magnetic fields are frozen-in the plasma, the kinetic Eq. (1) can be reduced to a transport equation for the isotropic part of the distribution function $N(\mathbf{r}, p, t)$. This approach can account for particle advection, diffusion and acceleration by the first-order Fermi mechanism in non-relativistic shocks. The diffusion coefficient in these analytical models is parameterized as $D(p) \propto r_g^a$, where the numerical index is generally in the range $0 \leq a \leq 2$. The widely used phenomenological *Bohm diffusion model* assumes $a = 1$, i.e., the mean free path $\Lambda(p) = \eta r_g(p)$, where the factor $\eta \geq 1$.

The CR current and anisotropy in the rest frame of a non-relativistic shock is $|\Delta_{1,m}| \sim v_s/c \ll 1$, where v_s is the shock velocity. The CR anisotropy can also be parameterized by the CR drift velocity v_{drift} relative to the background plasma in the rest frame of the upstream plasma. Various parameterizations of the CR current in DSA were used in recent studies of magnetic field amplification mechanisms by (e.g., Bell 2004, Pelletier et al. 2006, Amato and Blasi 2009, Luo and Melrose 2009) based on the CR transport equation. Monte Carlo simulations of DSA provide an alternative approach to the kinetic theory. In Monte Carlo techniques, particle scattering rates are parameterized as a function of energy and then the CR current (and other CR anisotropy moments) are derived in nonlinear shock models accounting for the CR backreaction on the plasma flow (e.g., Ellison et al. 1996, Vladimirov et al. 2006, 2008).

2.2 Resonant CR-streaming instability

Resonant interactions have long been known to amplify magnetic fluctuations on the scale of the CR gyroradius (e.g., Wentzel 1974, Zweibel 2003, Kulsrud 2005). The simplest case of interest for DSA is Alfvén wave amplification by streaming CRs. If the streaming speed of the cosmic rays through the ambient medium exceeds the Alfvén speed, then the amplitude of resonant Alfvén waves grows exponentially with time. The waves are emitted by the CR particles gyrating with gyrofrequency Ω as coherent cyclotron radiation. The resonance condition is $k v \cos(\vartheta) = \Omega$. This resonance condition is typical for DSA. The growth rate is positive if, in the wave frame, the particles stream in the opposite direction to the motion of the background fluid. Equivalently, the waves grow if, in the fluid frame, the mean streaming velocity of the particles

exceeds the wave velocity, i.e., $v_{\text{drift}} > v_{\text{ph}}$. The growth rate estimated by Blandford and Eichler (1987) is

$$\gamma^{\text{res}} \approx \Omega \left[\frac{v_{\text{drift}}}{v_{\text{ph}}} - 1 \right] \frac{n_{\text{cr}}}{n_{\text{a}}}, \quad (6)$$

where n_{cr} is the total number density of resonant cosmic rays and n_{a} is the background ion density.

2.3 Non-resonant streaming instabilities: short-scale

In addition to resonant amplification, the CR current can also efficiently amplify non-resonant magnetic fluctuations with scales smaller than the CR gyroradius (Bell 2004). The following two points are important to produce strong, short-scale turbulence.

(i) The cosmic-ray current has only a weak response to the fluctuations with scales shorter than the gyroradii, r_{g0} , of CR particles dominating the CR current (short-scale fluctuations), i.e., $kr_{g0} \gg 1$ (see discussion in section 2.1). In this case, the electric current of accelerated particles \mathbf{J}^{cr} is an external current in the momentum equation of the background plasma. The current is governed by sources of energetic particles and by local electromagnetic fields. The current \mathbf{J}^{cr} initiates a compensating return current in the background plasma.

(ii) The ponderomotive force of the CR current, $\mathbf{J}^{\text{cr}} \times \mathbf{B}/c$, is large enough to dominate the magnetic field tension in the momentum equation of the background plasma. Then the $\mathbf{J}^{\text{cr}} \times \mathbf{B}/c$ force from the CR current drives the Bell short-scale instability at scales below the CR gyroradius. This condition is satisfied for scales $k < k_1$ where

$$k_1 = \frac{4\pi J_0^{\text{cr}}}{c B_0}. \quad (7)$$

Note that the condition for mode growth, $r_{g0}k > 1$, together with Eq. (7), implies that the CR current that determines k_1 must be large enough to drive the non-resonant instability. The anisotropy of the relativistic particle distribution, $|\Delta_{1,0}|$, should exceed the ratio of the mean magnetic field energy density to the energetic particle energy density E_{cr} . That is

$$|\Delta_{1,0}| > \frac{B^2}{4\pi E_{\text{cr}}}, \quad (8)$$

where the CR current is given by $J_0^{\text{cr}} \approx |\Delta_{1,0}|en_{\text{cr}}c$.

Bell (2004, 2005) discovered that the system is unstable against linear perturbations that are $\propto \exp(\gamma t + i\mathbf{k}\mathbf{r})$ and the return current drives nearly purely growing modes. Here, γ is the linear growth rate.

In a cold plasma with sound speed a_0 , well below the Alfvén velocity v_a , the linear growth rate obtained by Bell (2005) depends only on the wavevector projection k_z on the local mean magnetic field, i.e.,

$$\gamma \approx \gamma_{\text{max}} k_z/k, \quad (9)$$

where

$$\gamma_{\max} = v_a \sqrt{k_1 |k| - k^2}. \quad (10)$$

According to the linear analysis of Bell (2005), the wavenumber of a growing mode must satisfy the condition $r_{g0}^{-1} < k < k_1$. Therefore, the instability growth rate is higher than the Alfvén frequency $v_a k$. The amplitudes of the growing mode in the linear approximation can be expressed as

$$|\mathbf{v}(\mathbf{k})|^2 \approx \frac{1}{4\pi\rho} \frac{k_1}{|k_z|} |\mathbf{b}(\mathbf{k})|^2, \quad (11)$$

provided that the kinetic energy density in the growing mode dominates over the magnetic energy density because $k_1 > k_z$. This is in contrast to Alfvén modes where the energy densities are equal.

The cold plasma approximation used in the analysis of Bell turbulence is valid if

$$\left(\frac{v_a}{v_{Ti}}\right)^2 > k_1 r_{g0} \frac{v_a}{c}, \quad (12)$$

where v_{Ti} is the thermal ion velocity. The approximation is typically good for galactic SNRs in a warm interstellar medium where the plasma parameter $\beta = a_0^2/v_a^2 \sim 1.0$. In the case of DSA by large-scale shocks in superbubbles (see e.g., Bykov and Toptygin 1993, 2001), or in hot intercluster plasma, the thermal corrections to the wave dispersion relations can be essential. A thorough discussion of the effects of a hot plasma on the short-scale modes was given by Zweibel and Everett (2010).

Particle-in-cell simulations by Riquelme and Spitkovsky (2009, 2010) showed that the back-reaction of the amplified field on CRs would limit the amplification factor of the Bell instability to less than a factor of about 10 in the upstream flows of galactic SNRs. The authors studied the possibility of further amplification driven near shocks by magnetized CRs, whose Larmor radii are smaller than the length scale of the field that was previously amplified by the Bell instability in the upstream flow. They found that additional amplification can occur due to the CR current perpendicular to the field. The maximum amplification of the instability is determined by the disruption of the CR current, which happens when CR Larmor radii in the amplified field become comparable to the length scale of the instability. Amplification factors up to ~ 45 were estimated in that case.

An important feature of the instability driven by the perpendicular current established by Riquelme and Spitkovsky (2010) is the characteristic dependence of the amplified field on the shock velocity, $B^2 \propto v_s^2$, which contrasts with the Bell instability acting alone where $B^2 \propto v_s^3$. Different scalings can, in principle, be constrained in statistical studies of radio SNRs, as done by Bandiera and Petruk (2010), but the results are sensitive to other parameters such as ambient density. It is also possible to constrain these scalings by comparing radio and X-ray synchrotron lightcurves of individual young supernova shells. In an amplified magnetic field, the synchrotron lightcurve will differ from the radio if strong magnetic field damping behind the shock occurs.

2.4 Non-resonant streaming instabilities: long-wavelength

The nonresonant, short-scale instability introduced by Bell (2004), and discussed in section 2.3, is fast and can strongly amplify short-scale magnetic field fluctuations. These strong, short-scale fluctuations are important for the dynamics of CR modified shocks and their emission properties, however, to study the maximum energies of CR particles in DSA one needs to study the amplification mechanisms for long-wavelength fluctuations of scales $r_{g0}k < 1$. Specifically, what are the consequences of long-wavelength fluctuations propagating in highly turbulent plasma with much shorter scale fluctuations? Also, contrary to the short-scale case, the response of the magnetized CR current on magnetic field fluctuations is not small in the limit $r_{g0}k < 1$.

Using a multi-scale, quasi-linear analysis, Bykov et al. (2011) showed that the presence of turbulence with scales shorter than the CR gyroradius enhances the growth of modes with scales longer than the gyroradius, at least for particular polarizations. They used a mean-field approach to average the equation of motion and the induction equation over the ensemble of magnetic field oscillations accounting for the anisotropy of relativistic particles on the background plasma. Bykov et al. (2011) derived the response of the magnetized CR current on magnetic field fluctuations and showed that, in the presence of short-scale Bell-type turbulence, long wavelength modes are amplified. In general, the growth rates depend on the mode propagation angle. For modes propagating parallel to the initial magnetic field, the growth rate is

$$\gamma^{lw}(k) \approx \sqrt{\frac{\pi N_B}{2}} \sqrt{\frac{kk_0}{\eta}} v_a, \quad (13)$$

and these modes have the fastest growth rates for the Bohm diffusion regime with $\eta \sim 1$.

The propagation angle θ_{\max} of the mode of maximum growth for $\eta > 1$ is

$$\cos \theta_{\max} = 1/\eta, \quad (14)$$

and the maximum growth rate at $\eta \gg 1$ is determined by

$$\gamma(k) \approx \sqrt{\frac{\pi N_B}{4}} \sqrt{kk_0} v_a. \quad (15)$$

The above results were obtained assuming $v_{\text{ph}}/v_s \ll 1$. In the case under consideration $\gamma(k) \sim \omega(k)$, and therefore from Eq. (15) one may get the validity condition in the form $\sqrt{\pi N_B/4} \sqrt{k_0/k} M_a^{-1} \ll 1$, where M_a is the Alfvén Mach number of the shock. The angular dependence of the growth rate in the hydrodynamical regime depends on the dimensionless collision strength η , as is shown in Fig. 1 of Bykov et al. (2011). The growth rates of resonant, non-resonant Bell's, and non-resonant long wavelength instabilities are illustrated in Fig. 2 taken from Bykov et al. (2011) where the polarization, helicity, and angular dependence of the growth rates are calculated for obliquely propagating modes for wavelengths both below and above the CR mean free path. The long-wavelength growth rates estimated for typical supernova remnant parameters are sufficiently fast to suggest a fundamental

increase in the maximum CR energy a given shock can produce. It should be noted that the phase velocity of the long-wavelength modes is a growing function of the wavelength and it is larger than the Alfvén speed. That may steepen the particle spectra at the highest energy end by reducing the effective shock compression at high energies. Also, the high phase velocity of the modes could increase the role of Fermi-II acceleration.

An important point is that the short-scale turbulence can influence the large-scale dynamics through the ponderomotive forces imposed on the plasma by the turbulence and the CR current. To derive the mean ponderomotive force one must average the momentum equation over the ensemble of short-scale fluctuations. When this is done, it is seen that the ponderomotive force due to the CR current response may result in a long-wavelength instability in a way somewhat similar to Bell’s instability.

2.5 Non-resonant firehose instability

The two CR streaming instabilities, resonant and non-resonant, despite being rather different physical mechanisms, both rely on the non-zero, first moment of the CR distribution, $\Delta_{1,m}$, i.e., the CR current. The anisotropic CR distributions, however, have non-vanishing higher order harmonics, $\Delta_{l,m}$. The well-known example of the instability due to the high-order anisotropy is the weakly magnetized thermal background plasma where the gas pressure anisotropy can be large. The systems we consider are known to be unstable if the anisotropy is large enough providing $P_{\parallel} > P_{\perp} + B^2/4\pi$ (firehose instability) or $P_{\perp} > P_{\parallel} + B^2/4\pi$ (mirror instability) (e.g., Treumann and Baumjohann 1997, and references therein), and can be important in astrophysical shocks (see, for example, Blandford and Eichler 1987, Blandford and Funk 2007). Since the growth rate is $\propto k[(P_{\parallel} - P_{\perp} - B^2/4\pi)/\rho]^{1/2}$, the instability operates in hot, high β plasmas.

In a strong supernova shock, the far upstream plasma is cold unless the SNR is located in a hot superbubble. Then, the free energy of the background plasma pressure anisotropy is not an efficient driver of magnetic field amplification. However, the CR pressure in the shock precursor close to the shock is expected to reach a sizeable fraction of the shock ram pressure, i.e., $P^{\text{CR}} = \zeta \rho_a v_s^2/2$. In this case, the anisotropy of the CR pressure defined by $\Delta_{2,m}$ should play a role. In the hydrodynamical regime, where the wavelength $2\pi/k$ is longer than the CR mean free path, Λ , the growth rate of the firehose instability can reach

$$\gamma^{fh}(k) \approx \sqrt{\zeta |\Delta_{2,0}|/2} v_s k \sim \sqrt{\zeta/2} \frac{v_s^2 k}{c}. \quad (16)$$

In this estimate, we assumed that $\Delta_{2,0} \propto \Delta_{1,0}^2$. However, as we have pointed out earlier, in some plasma flows with a complex structure of quasi-regular magnetic fields, or in the flows with regular or stochastic magnetic traps, one can expect much larger pressure anisotropy with $\Delta_{2,0} \propto \Delta_{1,0}$ and, therefore, higher growth rates. The mirror instability would occur with a growth rate similar to Eq. (16) if the perpendicular component of CR pressure dominates over the parallel pressure.

2.6 CR-pressure gradient driven acoustic instability

Drury and collaborators (Dorfi and Drury 1985, Drury and Falle 1986) showed that acoustic perturbations in a two-fluid plasma with a CR pressure gradient can grow if the scale of the CR gradient is shorter than D/a_0 , where a_0 is the thermal gas sound speed and D is the diffusion coefficient (see also Chalov 1988, Zank et al. 1990, Malkov and Drury 2001, Malkov et al. 2010). It is argued by Malkov and Diamond (2009) that this acoustic instability can be important for DSA. The growth rate of the acoustic instability can be estimated as

$$\gamma^{\text{ac}} \approx \frac{|\nabla P^{\text{CR}}|}{2\rho_a a_0} \quad (17)$$

for $k > \gamma^{\text{ac}}/a_0$ (see, e.g., Malkov et al. 2010, for a recent discussion). Since $|\nabla P^{\text{CR}}| \sim \zeta v_s^3/(\Lambda c a_0)$, then $k_{\text{min}} \sim \zeta(M_s^2 v_s/c)/\Lambda$. Thus, the long wavelength fluctuations of $k\Lambda < 1$ that are the most important to increase the maximum energies of CRs accelerated by DSA, can grow only if $\zeta(M_s^2 v_s/c) < 1$. This condition is rather restrictive for young SNRs in the warm interstellar medium. On the other hand, the short-scale fluctuations amplified by the instability are important for heating the plasma upstream of the shock and can contribute to the ponderomotive force discussed in section 2.4.

Beresnyak et al. (2009) proposed a DSA model in which stochastic magnetic fields in the shock precursor are amplified through small-scale dynamo effects. The solenoidal velocity perturbations that are required for the dynamo to work are produced in the model through the interactions of the pressure gradient of the CR precursor and the density perturbations in the inflowing fluid.

2.7 Instabilities in partially-ionized plasmas

The H_α emission from SN1006 and some other SNRs implies the presence of a sizable fraction of partially-ionized plasma in the circumstellar medium. Using a kinetic description of CRs, combined with a fluid description of the background plasma, Bykov and Topygin (2005) and Reville et al. (2007) investigated the growth of hydro-magnetic waves driven by CR streaming in the partially-ionized precursor environment of a supernova remnant shock. In this case, modifications of Ohm's law in the magnetized plasma can be important for the instability, as can ion-neutral damping. If the cosmic ray acceleration is efficient, large neutral fractions are required to compensate the growth of the non-resonant mode. For modest acceleration rates, the ion-neutral damping can dominate over the instability of weakly driven modes even at modest ionization fractions. In the case of a supernova shock interacting with a molecular cloud, such as in IC 443, W28, W44, or W51C, the low ionization in the ambient medium could limit the maximum energy of accelerated particles since this is largely determined by the upstream magnetic turbulence (e.g., Bykov et al. 2000). Observationally, SNRs interacting with molecular clouds are indeed found to be sources of high-energy gamma-ray emission (see e.g., Albert et al. 2007, Aharonian et al. 2008, Abdo et al.

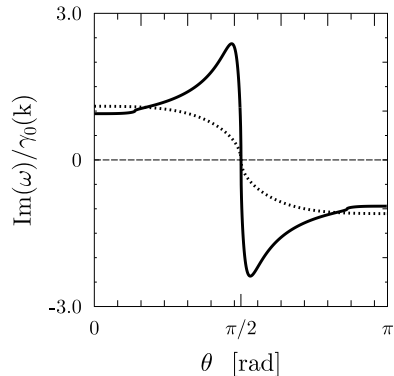


Fig. 1 The angular dependence of the growth rates of the long-wavelength unstable modes in the hydrodynamical regime where $kr_{g0} < \eta^{-1}$, for $\eta = 10$. The angle θ is between the wavevector and the CR current in the upstream rest frame of a parallel shock. The direction of the magnetic field determines the polarization (helicity) of the modes. The model parameters are $k_1 r_{g0} = 100$, the particle distribution index $\alpha = 4.0$, and the plasma parameter $\beta = a_0^2/v_a^2 = 1.0$. The solid and dot-dashed curves show the two unstable modes. The normalizing parameter γ_0 is determined by Eq. (13). See Bykov et al. (2011) for a comparison with the Bohm diffusion case $\eta = 1$

2010, Castro and Slane 2010). This emission is likely due to some combination of pion-decay and relativistic bremsstrahlung (e.g., Bykov et al. 2000, Uchiyama et al. 2010).

Charge exchange reactions in the downstream region, from neutrals crossing the shock and interacting, could result in a fast, cold ion beam. Ohira et al. (2009) presented a linear analysis of collisionless plasma instabilities between the cold beam and the hot downstream plasma. They found that, under SNR conditions, either the resonant instability or the Weibel-type instability are growing. The authors concluded that the mechanism may amplify the downstream magnetic field to more than $100 \mu\text{G}$, changing the shock structure and the synchrotron spectra and profiles. However, as we have pointed out *the turbulence amplification in the shock precursor* is the main factor determining the maximum CR energy and the efficiency of energy conversion to accelerated particles.

3 Magnetic field amplification in diffusive shock acceleration

The plasma instabilities in particle acceleration sources discussed above may result in magnetic turbulence and strong magnetic field amplification. The high efficiency of the acceleration means that nonlinear models are needed to predict the statistical characteristics of the amplified magnetic fields and their observational appearances. Diffusive shock acceleration models in su-

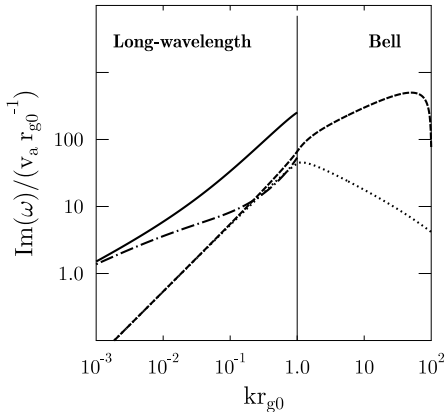


Fig. 2 The figure, from Bykov et al. (2010), shows growth rates of the parallel propagating modes as a function of the wavenumber to illustrate the effect of short-scale turbulence on the long-wavelength instability. The model parameters are $k_0 r_{g0} = 100$ and $\alpha = 4.0$. The solid and dot-dashed curves are simulated for two modes in the model with short-scale turbulence of $\xi = 5$ and $\eta = 10$ to demonstrate the behavior of the modes in the intermediate regime. For comparison, the dashed and dotted curves are calculated for the model without the short-scale turbulence, i.e., with $N_B = 0$ and $\eta \rightarrow \infty$ (c.f., Bell 2004).

pernova remnants imply wide dynamic ranges for the fluctuations and the particle momentum spectra extending for more than four decades. These wide dynamic ranges present a severe problem for the direct use of particle-in cell plasma simulations and some simplifications are required.

The nonlinear modeling of the short-scale Bell instability was done using MHD simulations (e.g., Bell 2004, Zirakashvili and Ptuskin 2008, Zirakashvili et al. 2008) assuming a fixed CR current as an external parameter. The MHD approach is justified since the CR current has only a weak response to the short-scale fluctuations. These models studied the spectral evolution in the short-scale range as well as the transformation of the turbulence through the subshock. The evolution of the Bell modes downstream from the shock was addressed by Pelletier et al. (2006), Marcowith et al. (2006), and Marcowith and Casse (2010).

A nonlinear Monte Carlo model of strong forward shocks in young supernova remnants with efficient particle acceleration, where a nonresonant instability driven by the CR current amplifies magnetic turbulence in the shock precursor, was developed by Vladimirov et al. (2009). Particle injection, magnetic field amplification, and the nonlinear feedback of particles and fields on the bulk flow were derived consistently in the Monte Carlo model as presented by Vladimirov et al. (2006, 2008). It was found that the shock structure depends critically on the efficiency of turbulence cascading. If cascading is suppressed, MFA is strong, the shock precursor is stratified, and the turbulence spectrum contains several discrete peaks. In Fig. 3, sim-

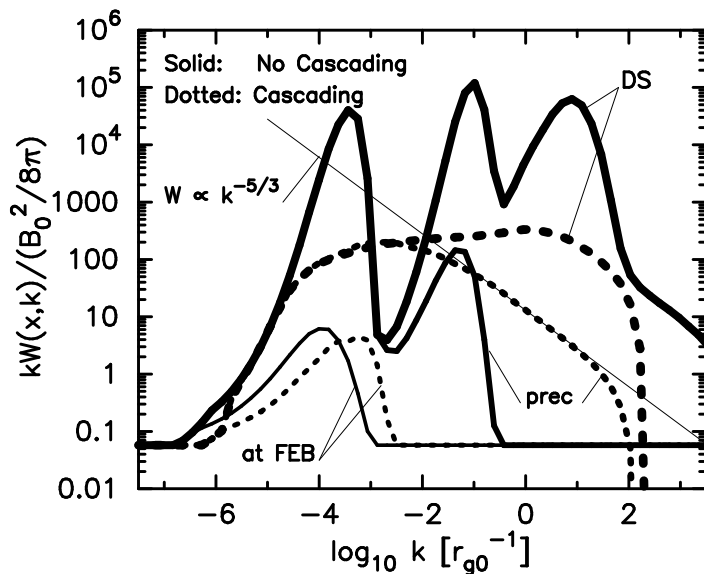


Fig. 3 Turbulence spectra, kW , at different locations relative to the subshock position as simulated by Vladimirov et al. (2009). The far upstream seed turbulence (at all k) is at the level indicated by the horizontal lines.

ulated turbulence spectra, kW , are shown at different locations relative to the subshock position.

In the solid curve, cascading is fully suppressed. In the dotted curve, the cascading from large to small scales is efficient and has the differential form corresponding to Kolmogorov's model. In the case with no cascading, the dissipation was assumed to be zero. With cascading, viscous dissipation was assumed. The peaks, apparent in the model with suppressed cascading, should influence synchrotron X-ray images of SNR shells, allowing observational tests of cascading and other assumptions intrinsic to the nonlinear model of nonresonant wave growth. In the next section, we discuss some models of X-ray synchrotron imaging of SNR shells.

Two opposite limits of cascading were considered in the model by Vladimirov et al. (2009) because our knowledge of turbulent cascading in collisionless plasmas is still very limited. It is limited, in part, because of the rather narrow dynamical range of the available nonlinear simulations. Information from direct measurements in the interplanetary medium can help constrain models of turbulent cascading, but this is also limited. The cascading of plasma wave spectra upstream of interplanetary shocks driven by coronal mass ejection events were analyzed by Bamert et al. (2008). They studied the competition between the upstream wave generation by suprathermal protons accelerated at the shock, and the cascading of wave energy in the inertial range of solar wind turbulence. Bamert et al. (2008) concluded that amplified solar wind turbulence upstream of interplanetary traveling shocks is better described by a Iroshnikov-Kraichnan-type cascade rather than the Kolmogorov-type.

The turbulent cascade is expected to be anisotropic, as is the case in the interplanetary medium (see e.g., Matthaeus et al. 1996, Horbury et al. 2008, Podesta 2009, and the references therein). Turbulent cascade dissipation will heat ions and electrons both in the upstream and downstream regions of the shock. Since the magnetic field amplification region in the shock precursor is of a finite size $\sim (c/v_s)\Lambda$, the upstream plasma temperature depends strongly on the heating rate and the plasma advection time. The cascade rate τ_c^{-1} depends on the field amplitude, growing mode polarization, and the plasma parameters. If $\tau_c^{-1}(c/v_s^2)\Lambda < 1$, the upstream plasma heating is inefficient. However, in the opposite limit with strong upstream turbulence, the plasma ion heating via an appropriate Landau resonance can be strong if the plasma parameter $\beta = a_0^2/v_a^2 > 1$. Electron heating is dominant in the highly magnetized upstream plasma if $\beta < 1$ (e.g., Quataert and Gruzinov 1999, Howes 2008). The Monte-Carlo simulations of the nonlinear structure of CR modified shocks by Vladimirov et al. (2008) demonstrated that the CR acceleration efficiency and the shock modification are sensitive to ion heating by the upstream turbulence. X-ray line emission from shocked shells of SNRs can be used to constrain the DSA models (e.g., Ellison et al. 2010).

There is an emerging class of SNRs, such as SN1006, RXJ1713.72-3946, Vela Jr, and others, that are *dominated* by non-thermal emission in X-rays, probably of synchrotron origin. Such emission results from electrons and/or positrons that are accelerated to well above TeV energies. Models of supernova shells show that these leptons radiate in strong magnetic fields and the radiation losses produce a marked cut off in the lepton spectrum. Figure 4 (from Ellison et al. 2010) shows the X-ray emission from RXJ1713.72-3946 as observed by the Suzaku spacecraft. This figure, and the models given in Ellison et al. (2010), indicate that the lack of thermal X-ray emission lines can be important for determining the origin of the non-thermal emission and the strength of the magnetic fields in the SNR. Since the amplified magnetic fields in DSA must be fluctuating, we next discuss the effect of fluctuations on the synchrotron images of SNRs.

4 Synchrotron images, spectra and polarization in supernova shells

Non-thermal emission in many sources of interest such as SNRs, gamma-ray bursts, and AGNs originates from synchrotron radiation of ultra-relativistic particles in turbulent magnetic fields. The effect of a random magnetic field on synchrotron images, emission spectra, and polarization can be very substantial.

4.1 Synchrotron mapping of twinkling supernova shells

It is instructive to illustrate first the effect of intermittency caused by the random magnetic field in terms of a power-law electron spectrum with spectral index Γ . The synchrotron emissivity $\tilde{I}(\mathbf{r}, t, \nu) \propto B^{(\Gamma+1)/2}$ shows that the local emissivity is relatively very high for large B and large Γ (a large Γ

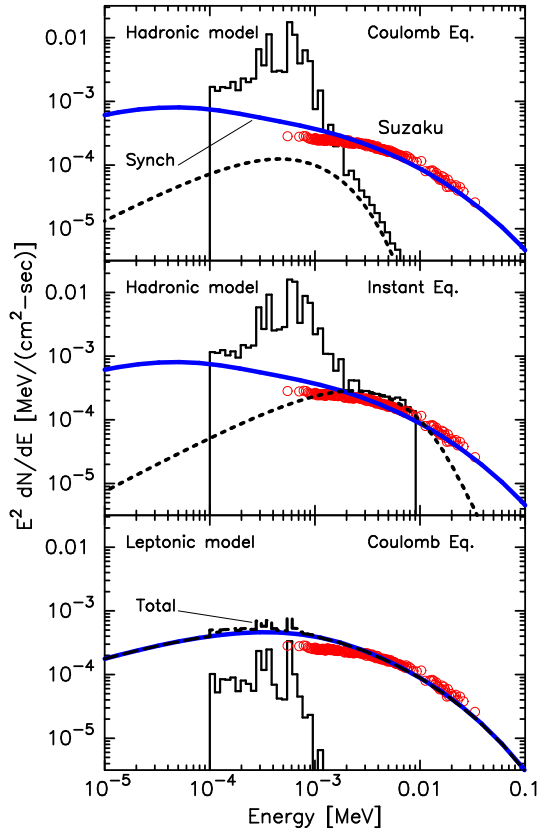


Fig. 4 The top two panels show fits to the *Suzaku* SNR J1713 observations with a hadronic model for both Coulomb and instant temperature equilibration but ignoring the X-line emission. The blue (heavy wt.) solid curve is the synchrotron continuum, the black solid curve is the thermal emission (only lines above 10^{-4} MeV are included), and the dotted curve is the underlying bremsstrahlung continuum. The observed emission would be the sum (not shown in the top two panels) of the solid black and blue curves. The bottom panel shows the leptonic model (with Coulomb equilibration) where parameters have been chosen to be consistent with the *Suzaku* observations. For the hadronic model, the radiation intensity is multiplied by 0.95 to match the observations. For the leptonic model, a normalization factor of 0.2 is required to match the observations. The *Suzaku* data have been adjusted for interstellar extinction so no extinction is applied to the model in this plot. See Ellison et al. (2010) for full details.

implies a steep spectrum). Therefore, the high-order statistical moments of the field dominate the synchrotron emissivity in the spectral cut-off regime and it is possible for a single strong local field maximum to produce a feature (dot or clump) that stands out on the map even after integrating the local emissivity over the line of sight. In lower energy maps, the contribution of a single maximum can be smoothed or washed out by contributions from a number of weaker field maxima integrated over the line of sight. A high-energy map, however, can be highly intermittent because the synchrotron

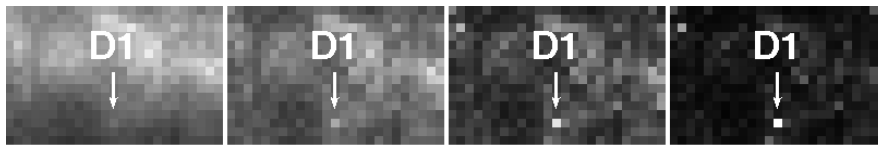


Fig. 5 Emission in the vicinity of a bright synchrotron dot D1 at different photon energies (see Bykov et al. 2008 for details). The four panels show, from left to right, $\nu^2 \cdot I(\mathbf{R}_\perp, t, \nu)$ maps of synchrotron emission at 0.5, 5, 20 and 50 keV, respectively.

emissivity depends on high-order moments of the random magnetic field at the cut-off frequency regime. The electron/positron spectra in the cut-off regime are usually exponential, and the exact shapes of the spectra dominated by synchrotron/Compton losses depend on the diffusion coefficient. A power-law approximation can only apply for a narrow electron energy range in the cut-off regime, where the effective spectral index Γ is increasing with the electron energy.

In order to calculate synchrotron emission maps and spectra, Bykov et al. (2008b) modeled a system of finite size, filled with a random magnetic field and electron spectra simulated with a DSA model accounting for synchrotron/Compton losses (see Bykov et al. 2000). A forward shock of spherical geometry was assumed in the image construction. The random field was composed of a superposition of magnetic fluctuations (plane waves) with random phases and a given spectrum of amplitudes. *Non-steady*, localized structures (dots, clumps and filaments), in which the magnetic field reaches exceptionally high values, typically arise in the statistically stationary random field sample. These non-steady magnetic field concentrations dominate the synchrotron emission (integrated along the line of sight) from the highest energy electrons in the cut-off regime of the electron distribution, resulting in an intermittent, twinkling, clumpy appearance even for a steady distribution of ultra-relativistic electrons. The spectral and temporal evolution of these high intensity synchrotron events, and the synchrotron images they produce, vary drastically at different photon energies.

In Figure 5 the synchrotron emission of a small region around a dot labeled D1 is shown for emission at 0.5, 5, 20 and 50 keV. There are observable differences in the synchrotron maps indicating that some features are bright at high energies and much less prominent at lower energies and vice versa. The physical reason for this difference comes from the fact that in the high-energy cut-off region of the electron spectrum, the local synchrotron emissivity depends strongly on the local field value as $B^{(\Gamma+1)/2}$, where the effective spectral index Γ is increasing with the photon energy in the cut-off spectral regime.

The simulated light curves of X-ray clumps may explain those observed in X-ray images of some supernova remnants by Uchiyama et al. (2007) and Patnaude and Fesen (2008). It is important to note that if the clumps are due to magnetic field intermittency, the time scale of their variation is not reflecting the ultra-relativistic electron loss time. The distinct characteristic of the modeled synchrotron emission is that its strong intermittency results directly from the exceptionally high magnetic field amplifications that

randomly occur. The peaks in synchrotron emission maps occur due to high-order moments of the magnetic field probability distribution function (PDF). Even if the PDF of projections of the local magnetic field are nearly Gaussian, the corresponding PDF of synchrotron peaks, simulated for a spatially homogeneous relativistic particle distribution, has strong departures from the Gaussian at large intensity amplitudes. This is because of the nonlinear dependence of the synchrotron emissivity on the local magnetic field in the high-energy cut-off regime of the electron spectrum. Intermittency of this nature, with very different appearances, is rather a common phenomenon in stochastic media (see e.g., Zel'dovich et al. 1987).

The models by Bykov et al. (2008b) and Bykov et al. (2009) make a few basic predictions. One is that the overall efficiency of synchrotron radiation from the cut-off regime in the electron spectrum can be strongly enhanced in a turbulent field with some value of $\sqrt{\langle B^2 \rangle}$, compared to emission from a uniform field, B_0 , where $B_0 = \sqrt{\langle B^2 \rangle}$. The second is that strong variations in the brightness of small structures can occur on time scales much shorter than variations in the underlying particle distribution. The variability time scale is shorter for higher energy synchrotron images. An estimate of the time scales of these intensity variations is consistent with the rapid time variability seen in some young SNRs by *Chandra*. The strong energy dependence predicted may be important for the future missions *NuSTAR*, *Astro-H* and others that will image SNR shells up to 50 keV.

4.2 Synchrotron X-ray Polarization in DSA

Synchrotron radiation in a regular, quasi-homogeneous magnetic field is polarized (e.g., Ginzburg and Syrovatskii 1965). It has long been known that random directions of magnetic fields, in addition to Faraday rotation, may strongly reduce the *average* polarization of synchrotron emission sources (e.g., Westfold 1959, Crusius and Schlickeiser 1986, Stroman and Pohl 2009). This explains the relatively low polarization frequently observed for radio synchrotron sources. However, as it was shown by Bykov et al. (2009), the turbulent magnetic fields that reduce the *average* polarization can result in highly polarized, intermittent, patchy structures potentially observable in high resolution X-ray images. In terms of a power-law electron spectrum with spectral index Γ , the degree of polarization is given by $\tilde{\Pi} \approx (\Gamma + 1)/(\Gamma + 7/3)$ and, therefore, $\tilde{\Pi}$ increases with Γ . Thus the synchrotron images will be highly polarized at high energies.

In order to construct maps of polarized synchrotron emission from SNR shells, it is convenient to use the local densities of the Stokes parameters (see e.g., Ginzburg and Syrovatskii 1965). Because of the additive property of the Stokes parameters \tilde{I} , \tilde{Q} , \tilde{U} , \tilde{V} for incoherent photons, we can integrate these weighted with the distribution function of radiating particles over the line of sight across the source. The degree of polarization is then determined in a standard way as $\Pi = \sqrt{Q^2 + U^2 + V^2}/I$. Starting from the simulated random magnetic-field, Bykov et al. (2009) have constructed maps of *polarized*

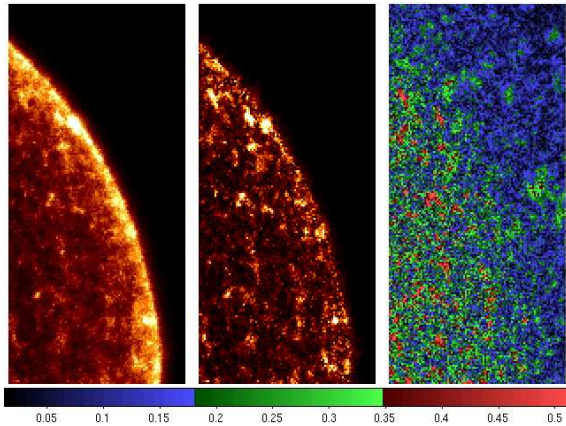


Fig. 6 Simulated maps of polarized synchrotron emission in a random magnetic field at 5 keV. Intensity, $\nu^2 \cdot I(\mathbf{R}_\perp, t, \nu)$, is shown with a linear color scale in the left panel. The central panel shows the product of intensity and polarization degree. The right panel shows the degree of polarization indicated by the color bar. The stochastic magnetic field sample has $\sqrt{\langle B^2 \rangle} = 3 \times 10^{-5}$ G and spectral index of magnetic fluctuations is $\delta = 1.0$ (from Bykov et al. (2009)).

X-ray emission of SNR shells. These are highly clumpy with polarizations up to 50% for energetic $> \text{TeV}$ electrons in the cut-off regime.

The detection of polarization in X-ray sources as faint as 1 milliCrab is an aim of the *Gravity and Extreme Magnetism Small Explorer (GEMS)* mission, recently selected for flight in 2014 by NASA. It will make a sensitive search for X-ray polarization using thin foil mirrors and Time Projection Chamber polarimeters with high efficiency in the 2-10 keV band (Kallman et al. 2010). The polarimeters under consideration, like *XPOL* aboard the planned *IXO* mission¹ and *POLARIX* proposed to measure X-ray polarization with an angular resolution of about 20 arcsec in a field of view of 15×15 arcmin with the minimum detectable polarization of 12% for a source of 1 mCrab within 100 ks of observing time (Costa et al. 2010), have good perspectives to detect polarized synchrotron emission from SNR shells.

The intermittent appearance of the polarized X-ray emission maps of young SNR shells can be studied in detail with imagers of a few arcsecond resolution, though even arcmin resolution images can provide important information as is illustrated in Fig. 6 (see Bykov et al. 2009). The polarized emission clumps of arcsecond scales are time variable on a year or longer (depending on the observed photon energy, magnetic field amplification factor, and the plasma density in the shell) allowing for rather long exposures even in the hard X-ray energy band. Hard X-ray observations in the spectral cut-off regime are the most informative to study the magnetic fluctuation spectra and the acceleration mechanisms of ultra-relativistic particles.

¹ <http://ixo.gsfc.nasa.gov/science/performanceRequirements.html>

5 Magnetic field amplification in star forming galaxies

The origin and evolution of magnetic field structures in galaxies is an important unsolved problem (e.g., Ruzmaikin et al. 1988, Rees 2006, Kulsrud and Zweibel 2008). Radio observations of the diffuse polarized radio emission from the disks of some spiral galaxies, as reviewed by Beck (2008), revealed large-scale coherent magnetic patterns that could be generated by dynamos, and dynamo models have been developed to explain the main observational features of the global magnetic fields of spiral galaxies (e.g., Ruzmaikin et al. 1988, Beck et al. 1996, Brandenburg and Subramanian 2005). In most galaxies, however, the field structure is more complicated. For example, radio synchrotron observations of nearby galaxies reveal dynamically important magnetic fields of 10-30 μG total strength in the spiral arms. These spiral arm fields, however, tend to have random orientations, while ordered fields (observed in radio polarization) are strongest in interarm regions and follow the orientation of the adjacent gas spiral arms.

A variety of observations (see Widrow 2002, for a review) suggest that magnetic fields are present in all galaxies including ellipticals and in galaxy clusters. Furthermore, it remains to be understood, in the context of the dynamo models, why well organized fields of surprisingly high strengths are observed in normal galaxies when the Universe was much younger than its present age (see e.g., Bernet et al. 2008, Wolfe et al. 2008).

5.1 Magnetic fields in irregular galaxies

Another issue to be addressed concerns the magnetic fields of dwarf irregular galaxies. Studies of magnetic fields in nearby dwarfs, as discussed recently by Chyzy (2010), revealed typically weak fields with the mean value of the total field strength about three times smaller than in normal spirals. The slow rotation rate in many irregular galaxies makes standard dynamo-type amplification of the magnetic field unlikely. On the other hand, dwarfs with stronger fields are associated with violent star-forming activity and these tend to be more massive and evolved systems. Their magnetic fields are thought to be regulated mainly by the surface density of the galactic star-formation rate (e.g., Chyzy 2010).

Star forming activity with clustered supernova explosions in superbubbles observed in galaxies (see e.g., Heiles 1990) may affect the mean magnetic field as suggested by Ferriere (1992). Moreover, numerical magnetohydrodynamical models by Siejkowski et al. (2010) of cosmic-ray driven dynamos in the interstellar medium of an irregular galaxy indicated the possibility of magnetic field amplification. The process of cosmic-ray acceleration may play a role in generating galactic magnetic fields at different stages of cosmic evolution. Non-resonant mechanisms of magnetic field amplification allow field enhancements on scales much larger than the gyroradii of the ultra-relativistic particles accelerated in the sources. Such fields amplified by the CR current and CR pressure anisotropy will have scales well above a parsec in the star forming regions, and well above a kiloparsec in clusters of galaxies. Observations of supernova remnants and galactic CRs suggest that there is

a high efficiency of conversion of the kinetic power of supernova shocks into CRs. Therefore, the specific mechanisms discussed above may convert a sizable fraction of the power released by SNRs into intermediate scale magnetic fields that are much larger than stellar scale fields. Some large-scale dynamo mechanism may also be necessary to produce the largest scale coherent fields seen in spiral galaxies.

5.2 Magnetic fields in the first generation Pop III supernova remnants

Simulations of nonlinear cosmic structure formation by Abel et al. (2002) and Xu et al. (2008) showed that the high-redshift analog of a molecular cloud is able to produce individual massive primordial stars, offering a natural explanation for the absence of purely metal free low mass stars in the Milky Way. The production of small-scale dynamos by turbulence created by accretion shocks during gravitational collapse may amplify initially weak magnetic fields in the protostellar cloud in the formation process of the first stars and galaxies (i.e., Schleicher et al. 2010). Massive stars exploding as supernovae provide energy, momentum, entropy, and metals at the very earliest stages of galactic evolution. Observations of high-redshift gamma-ray bursts likely indicate that relativistic particles and magnetic fields are produced during the collapse of massive primordial stars.

An important problem is whether there is a way to transfer a significant fraction of the high kinetic energy of the supernova ejecta into the magnetic fields of the remnant. The questions to be addressed are the following.

- (i) Can *collisionless* shocks be created by the supersonic ejecta in the very weakly magnetized plasma of $\beta \gg 1$?
- (ii) Can relativistic particles be accelerated in Pop III supernova remnants?
- (iii) Are there effective mechanisms of magnetic field amplification in Pop III supernova remnants?

Two-dimensional particle-in-cell simulations performed by Kato and Takabe (2010) to study weakly magnetized perpendicular shocks demonstrated the development of a *collisionless* shock with $\beta \approx 26$ (and an Alfvén Mach number of about 100). They showed that current filaments form in the foot region of the shock due to the ion-beam-Weibel instability (or the ion filamentation instability) and these filaments generated a strong magnetic field there. Strong fluctuating field generation is necessary in the standard paradigm of a collisionless shock since the only way to decelerate and thermalize the cold upstream flow is through the electromagnetic fields. In the downstream region, these current filaments also generated a tangled magnetic field that was about 15 times stronger than the upstream magnetic field. The shock simulations by Kato and Takabe (2010) reproduced well the Rankine-Hugoniot relations and indicated a substantial damping of the strong Weibel-type field fluctuations in the shock ramp (in the case of $\beta \approx 26$, the magnetic field contribution in the Rankine-Hugoniot relations is small). The authors noticed that a fraction of the ions are accelerated slightly on reflection at the shock.

If the temporal and spatial scales of the simulation were increased, it is expected that this fraction of reflected superthermal particles would continue to be accelerated by the Fermi-type DSA process. In this case, the magnetic field would continue to be amplified in a symbiotic relationship where the magnetic turbulence required to scatter and accelerate the CRs is created by the accelerated CRs themselves (e.g., Bell 2004, Vladimirov et al. 2008, Bykov et al. 2011). If this amplification operates as expected, a sizable fraction of the energy released by the supernova explosion can be transferred to energetic particles even with the initially weak magnetic field fluctuations of $B_0 \sim 0.1\text{-}1$ nG expected in the protostellar cloud.

The largest scale magnetic fluctuations amplified by the long wavelength non-resonant instabilities (that are discussed above in §2) can approach the scale of the shock. Therefore, the supernova remnant and its vicinity, with a scale size of about 30 pc, can be filled with a magnetic field of strength ~ 0.1 μG generated by instabilities driven by CR acceleration. The longest scale fields generated by the non-resonant CR instabilities in the shock *precursor* are in the collisional plasma regime since their wavelengths are longer than the Coulomb mean free path of the ambient thermal plasma. The long-wavelength fields should have, by many orders of magnitude, longer damping times than the short-lived Weibel-type fluctuations that are located just in a very narrow vicinity of the shock jump. The magnetic fields amplified in the SNR shock precursor can be considered as mesoscale fields since their scales are much larger than the stellar field sizes and larger than the CR gyroradii, but are below the observed largest scale coherent galactic magnetic fields in spiral galaxies presumably generated by galactic dynamos or by a global galactic CR current. The mesoscale fields can be the dominant fields in irregular galaxies and can be spread by the galactic winds through galactic groups and clusters. Furthermore, CR-driven winds in high-redshift galaxies may have important implications for the metal and magnetic field enrichment of the intergalactic medium (see e.g., Samui et al. 2010, Dubois and Teyssier 2010). In contrast, magnetic fields much lower than expected from CR instabilities were predicted in MHD simulations of the Biermann battery mechanism in the first generation of supernova remnants (i.e., Hanayama et al. 2009).

Magnetic field amplification by CRs produced by the first supernova explosions during the re-ionization epoch of the universe was discussed by (Miniati and Bell 2010). The CRs escape into the intergalactic medium carrying an electric current that results in magnetic field amplification. The authors found that magnetic fields are robustly generated throughout intergalactic space at a rate of $10^{-17} - 10^{-16}$ Gauss/Gyr, until the temperature of the intergalactic medium is raised by cosmic re-ionization. In another shock-related process, Ryu et al. (2008) discussed a scenario in which turbulent-flow motions are induced via the cascade of vorticity generated at cosmological shocks during the formation of large-scale structure. It was argued that this turbulent dynamo model might provide average magnetic field strengths of a few microgauss inside clusters and groups, approximately 0.1 μG around clusters and groups, and approximately 10 nG in filaments.

6 Discussion

Magnetic fields, both regular and stochastic, play a key role in charged particle accelerators providing both particle confinement and energy gain. The enormous energy release of gravitational (AGN, GRB, SNRs, clusters of galaxies, etc.) or thermonuclear origin (Type Ia SNRs, etc.), produces collisionless shocks and accelerates particles in many sources. It has long been known that strong shocks can only form in collisionless plasmas if magnetic turbulence is generated and some thermal particles are injected and accelerated to superthermal energies. The strong interrelation between shock formation and structure, magnetic turbulence, and energetic particles makes understanding the self-consistent production of magnetic turbulence in diffusive shock acceleration both essential and difficult.

While a great deal of progress has been made in this field, important challenges remain. In this brief review, we have discussed some recent work including resonant streaming and non-resonant CR-current driven instabilities. An important example of this is the Bell mechanism that efficiently amplifies short-scale turbulence by the CR current. Magnetic turbulence amplification may govern the nonlinear structure of CR-dominated flows, heat the upstream plasma, enhance synchrotron radiation, and limit high-energy electron energies. Furthermore, this mechanism might operate hand-in-hand with an instability for producing long-scale turbulence. The long-scale turbulence can be responsible for the highest energy particles accelerated by DSA. The basic DSA prediction that the highest energy accelerated ions can have a hard spectrum implies that the highest energy CRs may contain a sizeable fraction of the shock ram pressure. This implies that a consistent model of magnetic fields in the highly supersonic flow with accelerated particles is nonlinear and multi-scale.

The field of nonlinear shock acceleration is evolving rapidly with several prominent areas of active study. The long-wavelength instabilities discussed in Section 2 are yet to be combined with the resonant and short-wavelength instabilities in a nonlinear shock simulation. Such a combination will determine the relative importance of each and how the overall shock structure is influenced by them. The instabilities produced by escaping cosmic rays are only just now starting to be explored. Only with a consistent model combining the turbulence produced by escaping cosmic rays on the escaping cosmic rays themselves, can a reliable estimate of the maximum particle energy a given shock can produce be obtained.

In principle, the plasma physics of shock structure, magnetic turbulence, particle injection and acceleration, indeed, all aspects collisionless plasmas, can be determined with particle-in-cell (PIC) simulations. A great deal has been done in this field and we have mentioned a small fraction of this work in Section 2.3. The computational difficulties in producing PIC simulations with parameters close enough to systems such as SNRs are severe and we see future progress coming from synthesis of PIC models with semi-analytic and Monte Carlo techniques.

We have also discussed some recent work on the observational consequences of magnetic turbulence and synchrotron emission. The important

result is that fluctuating magnetic fields strongly modify the spectra of synchrotron emission in the case of steep electron spectra that are typical for X-ray emitting, TeV particles in young SNRs. X-ray images of synchrotron dominated SNR shells are predicted to be highly intermittent with polarized twinkling structures of different scales if the strong amplification of magnetic turbulence is indeed operating in DSA.

The current generation of X-ray telescopes – *Chandra* with its superb angular resolution and *XMM-Newton* with its high sensitivity – has uncovered a new world of synchrotron structures in young SNR shells. Further progress is certain to come from improved polarization and timing observations of SNRs at X-ray energies where the Faraday rotation is not essential and characteristic time scales are short enough. Observations at GeV-TeV energies are becoming more sensitive and theories of the highest energy cosmic rays must be improved accordingly. In all aspects of theory and observations, the turbulent magnetic field is the complicated glue tying things together.

Acknowledgements We thank the referee for a constructive comment. A.M.B. was supported in part by RBRF grants 09-02-12080 and by the RAS Presidium Programm, and the Russian government grant 11.G34.31.0001 to Sankt-Petersburg State Politechnical University. He performed some of the simulations at the Joint Supercomputing Centre (JSCC RAS) and the Supercomputing Centre at Ioffe Institute, St. Petersburg. D.C.E acknowledges support from NASA grants ATP02-0042-0006, NNH04Zss001N-LTSA, and 06-ATP06-21.

References

- Abdo AA, Ackermann M, Ajello M, Baldini L, et al. (2010) Observation of Supernova Remnant IC 443 with the Fermi Large Area Telescope. *Astrophys. J.* 712:459–468, 1002.2198
- Abel T, Bryan GL, Norman ML (2002) The Formation of the First Star in the Universe. *Science* 295:93–98, [arXiv:astro-ph/0112088](#)
- Achterberg A, Blandford RD, Reynolds SP (1994) Evidence for enhanced MHD turbulence outside sharp-rimmed supernova remnants. *Astron. Astrophys.* 281:220–230
- Aharonian F, Akhperjanian AG, Bazer-Bachi AR, Behera B, et al. (2008) Discovery of very high energy gamma-ray emission coincident with molecular clouds in the W 28 (G6.4-0.1) field. *Astron. Astrophys.* 481:401–410, 0801.3555
- Albert J, Aliu E, Anderhub H, Antoranz P, et al. (2007) Discovery of Very High Energy Gamma Radiation from IC 443 with the MAGIC Telescope. *Astrophys. J.* 664:L87–L90, 0705.3119
- Amato E, Blasi P (2009) A kinetic approach to cosmic-ray-induced streaming instability at supernova shocks. *Mon. Not. Royal Astron. Soc.* 392:1591–1600, 0806.1223
- Bamba A, Yamazaki R, Yoshida T, Terasawa T, et al. (2005) A Spatial and Spectral Study of Nonthermal Filaments in Historical Supernova Remnants: Observational Results with Chandra. *Astrophys. J.* 621:793–802, [arXiv:astro-ph/0411326](#)
- Bamba A, Yamazaki R, Yoshida T, Terasawa T, et al. (2006) Small-scale structure of non-thermal X-rays in historical SNRs. *Advances in Space Research* 37:1439–1442
- Bamert K, Kallenbach R, le Roux JA, Hilchenbach M, et al. (2008) Evidence for Iroshnikov-Kraichnan-Type Turbulence in the Solar Wind Upstream of Interplanetary Traveling Shocks. *Astrophys. J.* 675:L45–L48

-
- Bamert K, Kallenbach R, Ness NF, Smith CW, et al. (2004) Hydromagnetic Wave Excitation Upstream of an Interplanetary Traveling Shock. *Astrophys. J.* 601:L99–L102
- Bandiera R, Petruk O (2010) A statistical approach to radio emission from shell-type SNRs. I. Basic ideas, techniques, and first results. *Astron. Astrophys.* 509:A34+, 0911.0829
- Beck R (2008) Galactic and Extragalactic Magnetic Fields. In: American Institute of Physics Conference Series (ed. F A Aharonian, W Hofmann, & F Rieger), vol. 1085 of *American Institute of Physics Conference Series*, pp. 83–96, 0810.2923
- Beck R, Brandenburg A, Moss D, Shukurov A, et al. (1996) Galactic Magnetism: Recent Developments and Perspectives. *Ann. Rev. Astron. Astrophys.* 34:155–206
- Bell AR (2004) Turbulent amplification of magnetic field and diffusive shock acceleration of cosmic rays. *MNRAS* 353:550–558
- Bell AR (2005) The interaction of cosmic rays and magnetized plasma. *Mon. Not. Royal Astron. Soc.* 358:181–187
- Beresnyak A, Jones TW, Lazarian A (2009) Turbulence-Induced Magnetic Fields and Structure of Cosmic Ray Modified Shocks. *Astrophys. J.* 707:1541–1549, 0908.2806
- Berezinskii VS, Bulanov SV, Dogiel VA, Ginzburg VL, et al. (1990) Astrophysics of cosmic rays
- Bernet ML, Miniati F, Lilly SJ, Kronberg PP, et al. (2008) Strong magnetic fields in normal galaxies at high redshift. *Nature* 454:302–304, 0807.3347
- Blandford R, Eichler D (1987) Particle Acceleration at Astrophysical Shocks - a Theory of Cosmic-Ray Origin. *Phys Rep* 154:1–+
- Blandford R, Funk S (2007) The Magnetic Bootstrap. In: The First GLAST Symposium (ed. S Ritz, P Michelson, & C A Meegan), vol. 921 of *American Institute of Physics Conference Series*, pp. 62–64
- Brandenburg A, Subramanian K (2005) Astrophysical magnetic fields and nonlinear dynamo theory. *Phys Rep* 417:1–209, [arXiv:astro-ph/0405052](https://arxiv.org/abs/astro-ph/0405052)
- Butt YM, Porter TA, Katz B, Waxman E (2008) X-ray hotspot flares and implications for cosmic ray acceleration and magnetic field amplification in supernova remnants. *Mon. Not. Royal Astron. Soc.* 386:L20–L22, [arXiv:0801.4954](https://arxiv.org/abs/0801.4954)
- Bykov AM, Chevalier RA, Ellison DC, et al (2000) Nonthermal Emission from a Supernova Remnant in a Molecular Cloud. *Astrophys. J.* 538:203–216, [arXiv:astro-ph/0003235](https://arxiv.org/abs/astro-ph/0003235)
- Bykov AM, Dolag K, Durret F (2008a) Cosmological Shock Waves. *Space Sci. Rev.* 134:119–140, 0801.0995
- Bykov AM, Osipov SM, Ellison DC (2011) Cosmic ray current driven turbulence in shocks with efficient particle acceleration: the oblique, long-wavelength mode instability. *Mon. Not. Royal Astron. Soc.* 410:39–52, 1010.0408
- Bykov AM, Toptygin IN (1993) Particle Kinetics in Highly Turbulent Plasmas (Renormalization and Self-consistent Field Methods). *Physics-Uspexhi* 36:1020–1052
- Bykov AM, Toptygin IN (2001) A Model of Particle Acceleration to High Energies by Multiple Supernova Explosions in OB Associations. *Astronomy Letters* 27:625–633
- Bykov AM, Toptygin IN (2005) Generation of Magnetic Fluctuations Near a Shock Front in a Partially Ionized Medium. *Astronomy Letters* 31:748–754
- Bykov AM, Uvarov YA, Bloemen JBG, den Herder JW, et al. (2009) A model of polarized X-ray emission from twinkling synchrotron supernova shells. *Mon. Not. Royal Astron. Soc.* 399:1119–1125, 0907.2521
- Bykov AM, Uvarov YA, Ellison DC (2008b) Dots, Clumps, and Filaments: The Intermittent Images of Synchrotron Emission in Random Magnetic Fields of Young Supernova Remnants. *Astrophys. J.* 689:L133–L136, 0811.2498
- Cassam-Chenaï G, Hughes JP, Ballet J, Decourchelle A (2007) The Blast Wave of Tycho’s Supernova Remnant. *Astrophys. J.* 665:315–340, [arXiv:astro-ph/0703239](https://arxiv.org/abs/astro-ph/0703239)
- Cassam-Chenaï G, Hughes JP, Reynoso EM, Badenes C, et al. (2008) Morphological

- Evidence for Azimuthal Variations of the Cosmic-Ray Ion Acceleration at the Blast Wave of SN 1006. *Astrophys. J.* 680:1180–1197
- Castro D, Slane P (2010) Fermi Large Area Telescope Observations of Supernova Remnants Interacting with Molecular Clouds. *Astrophys. J.* 717:372–378, 1002.2738
- Chalov SV (1988) Instability of the structure of strong oblique MHD cosmic-ray shocks. *Astroph. Sp. Sci.* 148:175–187
- Chevalier RA (1977) Magnetic field amplification in interstellar collisionless shock waves. *Nature* 266:701–+
- Chyzy KT (2010) Magnetic fields in dwarfs versus early-type galaxies. *Highlights of Astronomy* 15:454–455
- Costa E, Bellazzini R, Tagliaferri G, Matt G, et al. (2010) POLARIX: a pathfinder mission of X-ray polarimetry. *Experimental Astronomy* :9–+
- Croston JH, Kraft RP, Hardcastle MJ, Birkinshaw M, et al. (2009) High-energy particle acceleration at the radio-lobe shock of Centaurus A. *Mon. Not. Royal Astron. Soc.* 395:1999–2012, 0901.1346
- Crusius A, Schlickeiser R (1986) Synchrotron radiation in random magnetic fields. *Astron. Astrophys.* 164:L16–L18
- Dorfi EA, Drury LO (1985) A cosmic ray driven instability. In: *International Cosmic Ray Conference* (ed. F C Jones), vol. 3 of *International Cosmic Ray Conference*, pp. 121–123
- Drury LO, Falle SAEG (1986) On the Stability of Shocks Modified by Particle Acceleration. *Mon. Not. Royal Astron. Soc.* 223:353–+
- Dubois Y, Teyssier R (2010) Magnetised winds in dwarf galaxies. *Astron. Astrophys.* 523:A72+, 0908.3862
- Ellison DC, Baring MG, Jones FC (1996) Nonlinear Particle Acceleration in Oblique Shocks. *Astrophys. J.* 473:1029–+, [arXiv:astro-ph/9609182](https://arxiv.org/abs/astro-ph/9609182)
- Ellison DC, Moebius E, Paschmann G (1990) Particle injection and acceleration at earth's bow shock - Comparison of upstream and downstream events. *Astrophys. J.* 352:376–394
- Ellison DC, Patnaude DJ, Slane P, Raymond J (2010) Efficient Cosmic Ray Acceleration, Hydrodynamics, and Self-Consistent Thermal X-Ray Emission Applied to Supernova Remnant RX J1713.7-3946. *Astrophys. J.* 712:287–293, 1001.1932
- Ferriere K (1992) Effect of the explosion of supernovae and superbubbles on the Galactic dynamo. *Astrophys. J.* 391:188–198
- Fryxell B, Kuranz CC, Drake RP, Grosskopf MJ, et al. (2010) The possible effects of magnetic fields on laser experiments of Rayleigh-Taylor instabilities. *High Energy Density Physics* 6:162–165
- Ginzburg VL, Syrovatskii SI (1964) *The Origin of Cosmic Rays*, New York: Macmillan
- Ginzburg VL, Syrovatskii SI (1965) Cosmic Magnetobremstrahlung (synchrotron Radiation). *Ann. Rev. Astron. Astrophys.* 3:297–+
- Hanayama H, Takahashi K, Tomisaka K (2009) Generation of Seed Magnetic Fields in Primordial Supernova Remnants. *ArXiv e-prints* 0912.2686
- Harvey-Smith L, Gaensler BM, Kothes R, Townsend R, et al. (2010) Faraday Rotation of the Supernova Remnant G296.5+10.0: Evidence for a Magnetized Progenitor Wind. *Astrophys. J.* 712:1157–1165, 1001.3462
- Heiles C (1990) Clustered supernovae versus the gaseous disk and halo. *Astrophys. J.* 354:483–491
- Helder EA, Vink J, Bassa CG, Bamba A, et al. (2009) Measuring the Cosmic-Ray Acceleration Efficiency of a Supernova Remnant. *Science* 325:719–, 0906.4553
- Horbury TS, Forman M, Oughton S (2008) Anisotropic Scaling of Magnetohydrodynamic Turbulence. *Physical Review Letters* 101(17):175 005–+, 0807.3713
- Howes GG (2008) Inertial range turbulence in kinetic plasmas. *Physics of Plasmas* 15(5):055 904–+, 0711.4358
- Jones FC, Ellison DC (1991) The plasma physics of shock acceleration. *Space Science Reviews* 58:259–346
- Jun B, Norman ML (1996) On the Origin of Radial Magnetic Fields in Young Supernova Remnants. *Astrophys. J.* 472:245–+, [arXiv:astro-ph/9606096](https://arxiv.org/abs/astro-ph/9606096)

-
- Kallman TR, Swank JH, GEMS Team (2010) The Gravity and Extreme Magnetism Small Explorer (GEMS). In: *Bulletin of the American Astronomical Society*, vol. 41 of *Bulletin of the American Astronomical Society*, pp. 737–+
- Kato TN, Takabe H (2010) Nonrelativistic Collisionless Shocks in Weakly Magnetized Electron-Ion Plasmas: Two-dimensional Particle-in-cell Simulation of Perpendicular Shock. *Astrophys. J.* 721:828–842, 1008.0265
- Kulsrud RM (2005) *Plasma physics for astrophysics*. Princeton University Press
- Kulsrud RM, Zweibel EG (2008) On the origin of cosmic magnetic fields. *Reports on Progress in Physics* 71(4):046 901–+, 0707.2783
- Luo Q, Melrose D (2009) Saturated magnetic field amplification at supernova shocks. *Mon. Not. Royal Astron. Soc.* 397:1402–1409, 0904.1038
- Malkov MA, Drury L (2001) Nonlinear theory of diffusive acceleration of particles by shock waves. *Reports on Progress in Physics* 64:429–481
- Malkov MA, Diamond PH (2009) Nonlinear Dynamics of Acoustic Instability in a Cosmic Ray Shock Precursor and its Impact on Particle Acceleration. *Astrophys. J.* 692:1571–1581
- Malkov MA, Diamond PH, Sagdeev RZ (2010) On the Structure and Scale of Cosmic Ray Modified Shocks. *ArXiv e-prints* 1007.3042
- Marcowith A, Casse F (2010) Postshock turbulence and diffusive shock acceleration in young supernova remnants. *Astron. Astrophys.* 515:A90+, 1001.2111
- Marcowith A, Lemoine M, Pelletier G (2006) Turbulence and particle acceleration in collisionless supernovae remnant shocks. II. Cosmic-ray transport. *Astron. Astrophys.* 453:193–202, [arXiv:astro-ph/0603462](https://arxiv.org/abs/astro-ph/0603462)
- Matthaeus WH, Ghosh S, Oughton S, Roberts DA (1996) Anisotropic three-dimensional MHD turbulence. *J. Geophys. Res.* 101:7619–7630
- Milne DK (1990) Polarization and magnetic fields in supernova remnants. In: *Galactic and Intergalactic Magnetic Fields* (ed. R Beck, R Wielebinski, & P P Kronberg), vol. 140 of *IAU Symposium*, pp. 67–72
- Miniati F, Bell AR (2010) Resistive Magnetic Field Generation at Cosmic Dawn. *ArXiv e-prints* 1001.2011
- Ohira Y, Terasawa T, Takahara F (2009) Plasma Instabilities as a Result of Charge Exchange in the Downstream Region of Supernova Remnant Shocks. *Astrophys. J.* 703:L59–L62, 0908.3369
- Patnaude DJ, Fesen RA (2008) Proper Motions and Brightness Variations of Non-thermal X-ray Filaments in the Cassiopeia A Supernova Remnant. *ApJ* (submitted) *ArXiv* 08080692 808, 0808.0692
- Pelletier G, Lemoine M, Marcowith A (2006) Turbulence and particle acceleration in collisionless supernovae remnant shocks. I. Anisotropic spectra solutions. *Astron. Astrophys.* 453:181–191, [arXiv:astro-ph/0603461](https://arxiv.org/abs/astro-ph/0603461)
- Petruk O, Dubner G, Castelletti G, et al (2009) Aspect angle for interstellar magnetic field in SN 1006. *Mon. Not. Royal Astron. Soc.* 393:1034–1040, 0811.2319
- Podesta JJ (2009) Dependence of Solar-Wind Power Spectra on the Direction of the Local Mean Magnetic Field. *Astrophys. J.* 698:986–999, 0901.4940
- Pohl M, Yan H, Lazarian A (2005) Magnetically Limited X-Ray Filaments in Young Supernova Remnants. *Astrophys. J.* 626:L101–L104
- Ptuskin V, Zirakashvili V, Seo E (2010) Spectrum of Galactic Cosmic Rays Accelerated in Supernova Remnants. *Astrophys. J.* 718:31–36, 1006.0034
- Quataert E, Gruzinov A (1999) Turbulence and Particle Heating in Advection-dominated Accretion Flows. *Astrophys. J.* 520:248–255, [arXiv:astro-ph/9803112](https://arxiv.org/abs/astro-ph/9803112)
- Rees MJ (2006) Origin of cosmic magnetic fields. *Astronomische Nachrichten* 327:395–+
- Reville B, Kirk JG, Duffy P, O’Sullivan S (2007) A cosmic ray current-driven instability in partially ionised media. *Astron. Astrophys.* 475:435–439, 0707.3743
- Reynolds SP (2008) Supernova Remnants at High Energy. *Ann. Rev. Astron. Astrophys.* 46:89–126
- Riquelme MA, Spitkovsky A (2009) Nonlinear Study of Bell’s Cosmic Ray Current-Driven Instability. *Astrophys. J.* 694:626–642, 0810.4565
- Riquelme MA, Spitkovsky A (2010) Magnetic Amplification by Magnetized Cosmic

- Rays in Supernova Remnant Shocks. *Astrophys. J.* 717:1054–1066, 0912.4990
- Ruzmaikin AA, Sokolov DD, Shukurov AM (eds.) (1988) Magnetic fields of galaxies, vol. 133 of *Astrophysics and Space Science Library*
- Ryu D, Kang H, Cho J, Das S (2008) Turbulence and Magnetic Fields in the Large-Scale Structure of the Universe. *Science* 320:909–, 0805.2466
- Samui S, Subramanian K, Srianand R (2010) Cosmic ray driven outflows from high-redshift galaxies. *Mon. Not. Royal Astron. Soc.* 402:2778–2791, 0909.3854
- Schleicher DRG, Banerjee R, Sur S, Arshakian TG, et al. (2010) Small-scale dynamo action during the formation of the first stars and galaxies. I. The ideal MHD limit. *Astron. Astrophys.* 522:A115+, 1003.1135
- Schlickeiser R (2002) *Cosmic Ray Astrophysics*. Springer, Berlin
- Schure KM, Vink J, Achterberg A, Keppens R (2009) Evolution of Magnetic Fields in Supernova Remnants. In: *Revista Mexicana de Astronomia y Astrofisica Conference Series*, vol. 36 of *Revista Mexicana de Astronomia y Astrofisica Conference Series*, pp. 350–+, 0810.5150
- Siejkowski H, Soida M, Otmianowska-Mazur K, Hanasz M, et al. (2010) Cosmic-ray driven dynamo in the interstellar medium of irregular galaxies. *Astron. Astrophys.* 510:A97+, 0909.0926
- Stone JM, Gardiner T (2007) The Magnetic Rayleigh-Taylor Instability in Three Dimensions. *Astrophys. J.* 671:1726–1735, 0709.0452
- Stroman W, Pohl M (2009) Radio polarimetry signatures of strong magnetic turbulence in Supernova Remnants. *ArXiv e-prints* 0902.1701
- Toptygin IN (1985) Cosmic rays in interplanetary magnetic fields
- Treumann RA, Baumjohann W (1997) *Advanced space plasma physics*
- Uchiyama Y, Aharonian FA, Tanaka T, et al (2007) Extremely fast acceleration of cosmic rays in a supernova remnant. *Nature* 449:576–578
- Uchiyama Y, Blandford R, Funk S, Tajima H, et al. (2010) Gamma-ray Emission from Crushed Clouds in Supernova Remnants. *ArXiv e-prints* 1008.1840
- Vink J (2008) . In: *AIP Conference Series* (ed. F A Aharonian et al), vol. 1085, p. 169
- Vink J, Laming JM (2003) On the Magnetic Fields and Particle Acceleration in Cassiopeia A. *Astrophys. J.* 584:758–769, [arXiv:astro-ph/0210669](#)
- Vladimirov A, Ellison DC, Bykov A (2006) Nonlinear Diffusive Shock Acceleration with Magnetic Field Amplification. *Astrophys. J.* 652:1246–1258, [arXiv:astro-ph/0606433](#)
- Vladimirov AE, Bykov AM, Ellison DC (2008) Turbulence Dissipation and Particle Injection in Nonlinear Diffusive Shock Acceleration with Magnetic Field Amplification. *Astrophys. J.* 688:1084–1101, 0807.1321
- Vladimirov AE, Bykov AM, Ellison DC (2009) Spectra of Magnetic Fluctuations and Relativistic Particles Produced by a Nonresonant Wave Instability in Supernova Remnant Shocks. *Astrophys. J.* 703:L29–L32, 0908.2602
- Wentzel DG (1974) Cosmic-ray propagation in the Galaxy - Collective effects. *Ann Rev Astron Astroph* 12:71–96
- Westfold KC (1959) The Polarization of Synchrotron Radiation. *Astrophys. J.* 130:241–+
- Widrow LM (2002) Origin of galactic and extragalactic magnetic fields. *Reviews of Modern Physics* 74:775–823, [arXiv:astro-ph/0207240](#)
- Wolfe AM, Jorgenson RA, Robishaw T, Heiles C, et al. (2008) An 84- μ G magnetic field in a galaxy at redshift $z = 0.692$. *Nature* 455:638–640, 0811.2408
- Xu H, O’Shea BW, Collins DC, Norman ML, et al. (2008) The Biermann Battery in Cosmological MHD Simulations of Population III Star Formation. *Astrophys. J.* 688:L57–L60, 0807.2647
- Zank GP, Axford WI, McKenzie JF (1990) Instabilities in energetic particle modified shocks. *Astron. Astrophys.* 233:275–284
- Zel’dovich YB, Molchanov SA, Ruzmaikin AA, Sokoloff DD (1987) Intermittency in random media. *Sov Physics-Uspexhi* 30:353–369
- Zirakashvili VN, Ptuskin VS (2008) Diffusive Shock Acceleration with Magnetic Amplification by Nonresonant Streaming Instability in Supernova Remnants. *Astrophys. J.* 678:939–949, 0801.4488

- Zirakashvili VN, Ptuskin VS, Völk HJ (2008) Modeling Bell's Nonresonant Cosmic-Ray Instability. *Astrophys. J.* 678:255–261, 0801.4486
- Zweibel EG (2003) Cosmic-Ray History and Its Implications for Galactic Magnetic Fields. *Astrophys. J.* 587:625–637, [arXiv:astro-ph/0212559](https://arxiv.org/abs/astro-ph/0212559)
- Zweibel EG, Everett JE (2010) Environments for Magnetic Field Amplification by Cosmic Rays. *Astrophys. J.* 709:1412–1419, 0912.3511